VOLUME 118, NUMBER 17
MAY 1, 1996

JOURNAL OF THE AMERICAN CHEMICAL SOCIETY

NMR Studies of a $^{13}C,^{15}N$-Labeled G_{M4}-Lactam Glycolipid at an Oriented Model-Membrane Interface

Brian A. Salvatore, Ranajeet Ghose, and James H. Prestegard*

Contribution from the Department of Chemistry, Yale University, New Haven, Connecticut 06520-8107

Received December 4, 1995[⊗]

Abstract: Liquid crystal NMR techniques were used to study an isotopically labeled lactam analog of ganglioside G_{M4} in an oriented bilayer system composed of *L*-α-dimyristoylphosphatidylcholine (DMPC) and 3-((cholamidopropyl)-dimethylammonio)-2-hydroxy-1-propanesulfonate (CHAPSO). This discoidal bilayer system is used to mimic a biological membrane, the natural environment of G_{M4} and other glycolipids. Residual dipolar couplings ($^{13}C-^{13}C$ and $^{15}N-^{13}C$) and chemical shift anisotropy effects for the amide ^{13}C and ^{15}N labeled sites were measured in G_{M4} lactam, using both one- and two-dimensional NMR methods. The dipolar coupling data were interpreted using a torsional search for preferred geometry about the two elements of the glycosidic bond attaching the headgroup to the bilayer surface. This yielded three independent families of structures, all of which were consistent with the dipolar coupling data. An order matrix analysis was used to compare experimentally measured changes in chemical shifts upon orientation to those predicted by chemical shift tensors derived from *ab initio* calculations. One of the three families of structures was readily eliminated based on chemical shift measurements, and another was eliminated based on energetic considerations, leaving a single structure to represent the average conformation of the G_{M4} lactam headgroup at a membrane surface.

Introduction

The conformational study of membrane-bound oligosaccharides is an area of significant interest, since these molecules are known to serve as recognition elements for many extracellular proteins and are involved in autoimmune disorders, cancer metastasis, and cell differentiation.[1] To address this interest, NMR methods for the study of such molecules in an environment that resembles their natural membrane-bound state have been developed over recent years.[2] The methods employ a field-orientable liquid crystalline system composed of discoidal phospholipid-based micelles [*L*-α-dimyristoylphosphatidylcholine (DMPC)/3-((cholamidopropyl)dimethylammonio)-2-hydroxy-1-propanesulfonate (CHAPSO) 3:1]. This system allows the measurement of residual dipolar couplings as well as changes in the chemical shifts upon orientation. From these measurements, conformational information can be derived. Previous work has been limited to NMR spin systems containing ^{13}C, ^{1}H, and ^{2}H nuclei.[3] Here we extend this work to a four-atom spin system composed of three ^{13}C sites and one ^{15}N site in a synthetically produced G_{M4} lactam, an analog of a naturally-occurring ganglioside lactone.[4]

Gangliosides are sialic acid containing glycosphingolipids. Their presence in the brain, in myelin fibers,[5] and on nerve cells[6]

[⊗] Abstract published in *Advance ACS Abstracts,* April 1, 1996.

(1) (a) Lee, Y. C.; Lee, R. T. *Acc. Chem. Res.* **1995**, *28*, 321−327. (b) Sharon, N.; Lis, H. *Sci. Am.* **1993**, *268*, 82−89. (c) Chu, J. W. K.; Sharom, F. J. *Cell. Immunol.* **1991**, *132*, 319−338. (d) Shimada, K.; Koh, C.-S.; Uemura, K.-I.; Yanagisawa, N. *Cell. Immunol.* **1994**, *154*, 231−239.

(2) Sanders, C. R., II; Hare, B. J.; Howard, K. P.; Prestegard, J. H. *Prog. Nuc. Mag. Res. Spectr.* **1994**, *26*, 421−444.

(3) (a) Howard, K. P.; Prestegard, J. H. *J. Am. Chem. Soc.* **1995**, *117*, 5031−5040. (b) Tyrell, P. M.; Prestegard, J. H. *J. Am. Chem. Soc.* **1986**, *108*, 3990−3995. (c) Aubin, Y.; Prestegard, J. H. *Biochemistry* **1993**, *32*, 3422−3428. (d) Ram, P.; Prestegard, J. H. *J. Am. Chem. Soc.* **1988**, *110*, 2383−2388. (e) Hare, B. J.; Howard, K. P.; Prestegard, J. H. *Biophys. J.* **1993**, *64*, 392−398.

S0002-7863(95)04048-0 CCC: $12.00

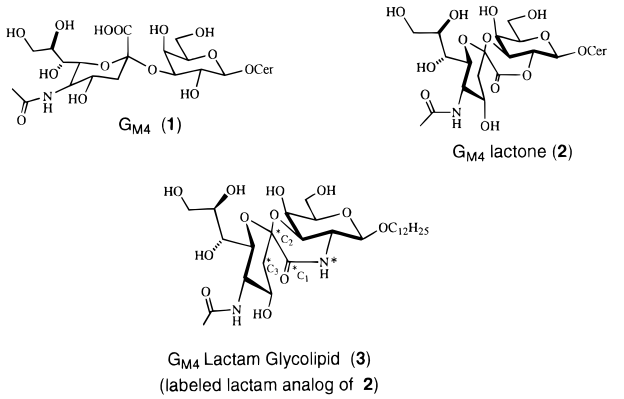

Figure 1. G_{M4} lactam (**1**), one of the two naturally-occurring G_{M4} lactones (**2**), and a G_{M4} lactam glycolipid (**3**) analog of lactone **2**. Cer is an abbreviation for ceramide, the lipid anchor found in naturally-occurring gangliosides. Asterisks (*) indicate sites of isotopic enrichment (>98%).

has been well documented. They are also believed to modulate growth factor receptor interactions, thereby regulating cell growth.[7] Their overexpression in certain cancer cells has also been well-established.[8] Thus, they are potential antigens for use in the development of cancer vaccines.[9] Ganglioside shedding from malignant cells is also believed to be a major cause of the extreme immunosuppression seen in late-stage cancer patients.[10] Capitalizing on beneficial aspects and blocking detrimental effects of gangliosides depends, to some extent, on a better understanding of conformational properties. Work toward understanding the conformational behavior on a molecular level, however, requires new techniques applicable in the special environment in which these molecules normally function.

The actual molecule to be studied here, G_{M4} lactam, is a direct analog of G_{M4} lactone. Two G_{M4} lactones have been recently isolated from whale brain and were shown to be natural compounds.[11] However, these lactones are subject to hydrolysis in an aqueous environment. Magnusson and co-workers reported G_{M4} lactam to be a hydrolytically stable analog of the G_{M4} lactone.[4a] These workers have used both proton−proton-NOEs and scalar coupling constants to demonstrate that ganglioside lactams are, in general, conformationally similar to the corresponding lactones.[4]

We have recently completed the total synthesis of a ^{13}C, ^{15}N-labeled glycolipid analog of one of the G_{M4} lactones (Figure 1).[12] This is both a biochemically and spectroscopically interesting target for conformational analysis. The four-atom NMR spin system (>98% isotopic enrichment) is localized in the conformationally rigid headgroup of this molecule and provides a wealth of residual dipolar couplings and chemical shift offset effects. These can be analyzed in terms of the molecule's conformational preference about the single pair of ϕ and ψ torsions which connect the headgroup to its membrane anchor.

The dipolar interaction between two spin 1/2 nuclei in a rigid fragment is dependent on a set of fixed properties which includes the gyromagnetic ratios (γ) of the interacting nuclei and the internuclear distance (r). It also depends on an angular factor which is averaged by motion to yield the observed (residual) dipolar couplings in the liquid crystal micelle system. To provide a convenient molecular picture of structure and motion, we prefer to break the effects of this averaging into three parts. These are represented in the expression for the residual dipolar contribution to the splitting, D_{ij} given below. S_{micelle} describes the orientation and order of the bilayer fragments themselves and can usually be evaluated from the observed scaling of ^{31}P and carbonyl ^{13}C chemical shifts of the phospholipids in the bilayer matrix (here, ca. −0.23). S_{axial} accounts for just axially symmetric motion about the bilayer normal of the membrane anchor (the alkyl chain attached to the glycosidic oxygen of G_{M4} galactose in our case). Additional averaging due to motions about the glycosidic torsions are represented by the brackets surrounding the angular term where θ_{ij} is the angle between internuclear vector$_{ij}$ and the alkyl chain axis.

$$D_{ij} = \frac{-\gamma_i \gamma_j h}{2\pi^2 r^3} S_{\text{micelle}} S_{\text{axial}} \left\langle \frac{3\cos^2 \theta_{ij} - 1}{2} \right\rangle \qquad (1)$$

Modeling of motion about the glycosidic angles can be accomplished by choosing ϕ and ψ and allowing uniform sampling of conformers in torsional wells of widths $\Delta\phi$ and $\Delta\psi$. S_{axial}, ϕ, ψ, $\Delta\phi$, and $\Delta\psi$ may be searched to find a set of values which simultaneously fit all of the measured dipolar couplings.

It is also possible to obtain additional information about the orientational properties of molecules by measuring chemical shift anisotropy effects. The chemical shift observed in an oriented system can be expressed as

$$\langle \delta_{\text{obs}} \rangle = \frac{1}{3}(\delta_{11} + \delta_{22} + \delta_{33}) + \delta_{\text{an}} \qquad (2)$$

where δ_{ij} are the diagonal elements of the shift tensor. Note that this expression contains an anisotropic contribution (δ_{an}). For an isotropically tumbling molecule, the anisotropic contributions average to zero, and only the isotropic shift remains. However, in an anisotropic system, changes in the observed chemical shift upon orientation contain additional information about order and conformation. The offset of the observed chemical shift from its isotropic value can be expressed as

$$\langle \delta_{\text{an}} \rangle = -\frac{2}{3} S_{\text{micelle}} \sum_{i,j} \delta_{ij} S_{ij} \qquad (3)$$

where δ_{ij} are the elements of the chemical shift tensor in a molecular frame of reference, S_{micelle} is the same order parameter which occurred in our dipolar expression, and S_{ij} are the elements of an order tensor that includes the effects of S_{axial} and ϕ, ψ averaging. This is an alternate way of representing the averaging included in S_{axial} and within the brackets of eq 1.

(4) (a) Magnusson, G.; Wilstermann, M.; Ray, A. K.; Nilsson, U. In *Synthetic Oligosaccharides*; Kovac, P., Ed.; ACS Symposium Series 560, American Chemical Society, Washington, DC, 1994; pp 233−248. (b) Ray, A. K.; Nilsson, U.; Magnusson, G. *J. Am. Chem. Soc.* **1992**, *114*, 2256−2257.

(5) (a) Saito, M.; Yu, R. K. *J. Neurochem.* **1992**, *58*, 83−87. (b) Yu, R. K.; Macala, L. J.; Farooq, M.; Sbaschnig-Agler, M.; Norton, W. T.; Ledeen, R. W. *J. Neurosci. Res.* **1989**, *23*, 136−141. (c) Farrer, R. G.; Benjamins, J. A. *J. Neurochem.* **1992**, *58*, 1477−1484.

(6) Svennerholm, L.; Boström, K.; Fredman, P.; Jungbjer, B.; Lekman, A.; Månsson, J.-E.; Rynmark, B.-M. *Biochim. Biophys. Acta* **1994**, *1214*, 115−123.

(7) (a) Feizi, T.; Childs, R. A. *TIBS* **1985**, *10*, 24−29. (b) Feizi, T. *Nature* **1985**, *314*, 53−57.

(8) (a) Hakomori, S. *Cancer Res.* **1985**, *45*, 2405−2414. (b) Hakomori, S. *Curr. Biol.* **1991**, *3*, 646−653.

(9) (a) Livingston, P. O. *Curr. Biol.* **1992**, *4*, 624−629. (b) Livingston, P. O.; Natoli, E. J.; Calves, M. J.; Stockert, E.; Oettgen, H. F.; Old, L. J. *Proc. Natl. Acad. Sci. U.S.A.* **1987**, *84*, 2911−2915.

(10) (a) Ladisch, S. Hasegawa, A.; Li, R.; Kiso, M. *Biochemistry* **1995**, *34*, 1197−1202. (b) Ladisch, S.; Becker, H.; Ulsh, L. *Biochim. Biophys. Acta* **1992**, *1125*, 180−188.

(11) Terabayashi, T.; Ogawa, T.; Kawanishi, Y. *J. Biochem.* **1990**, *107*, 868−871.

(12) Salvatore, B. A.; Prestegard, J. H., manuscript in preparation.

More specifically

$$S_{\text{axial}}\left\langle\frac{3\cos^2\theta-1}{2}\right\rangle = \cos^2\phi_x(-S_{yy}-S_{zz}) + \cos^2\phi_y S_{yy} + \cos^2\phi_z S_{zz} + 2\cos\phi_x\cos\phi_y S_{xy} + 2\cos\phi_x\cos\phi_z S_{xz} + 2\cos\phi_y\cos\phi_z S_{yz} \quad (4)$$

where the ϕ_i are the angles between the head group's fixed order tensor axes and the internuclear vectors. The five independent order tensor elements (S_{ij}) can thus be evaluated from dipolar coupling data in a manner analogous to that described above for ϕ, ψ, $\Delta\phi$, $\Delta\psi$, and S_{axial}, and these elements may then be used to predict anisotropic contributions to chemical shift. Agreement of the predictions based on S_{ij} from dipolar data with experiment can thus be used to screen structural models.

Materials and Methods

DMPC and CHAPSO were purchased from Sigma. Labeled G_{M4} lactam was prepared by total synthesis as reported elsewhere.[12] Liquid crystal NMR samples were prepared by combining G_{M4} lactam (6.5 mg), DMPC (86 mg), and CHAPSO (26.5 mg) in 250 μL of deionized water and 28.5 μL D_2O. Sample preparation involves several brief cooling (0 °C) and warming (60 °C) cycles with intermittent mixing through low-speed centrifugation to achieve homogeneity.

^{13}C-NMR spectra of oriented samples were acquired on Bruker AM-500 and GE Omega-500 spectrometers at 125.8 MHz. Most chemical shift offsets and dipolar couplings could be measured directly from 1D-^{13}C spectra. ^{13}C chemical shifts were referenced relative to 54.0 ppm for the sharp signal from the CHAPSO cholamido-methyl group. Proton homonuclear and heteronuclear decoupling were accomplished using WALTZ-16 (Bruker) and GARP-1 (GE-Omega). Proton decoupler power was high (20−40 W), acquisition times in 1D ^{13}C-experiments were typically short (90 ms), and the relaxation delays were typically 2.5 s. The S_{micelle} term was measured from ^{31}P NMR spectra taken on a GE Omega-300 spectrometer at 75 MHz. The isotropic ^{15}N chemical shift was measured directly, using a 10 mm broad-band probe with ^1H-decoupling on a Bruker AM-500. Isotropic and oriented ^{15}N chemical shifts were referenced relative to a standard consisting of 2.9 *M* NH_4Cl in 1.0 *M* HCl (24.93 ppm).[13]

The oriented liquid crystal samples were equilibrated in the magnet for at least 15 min prior to acquisition at a temperature where formation of an ordered liquid crystal is known to occur. In a few cases, it was necessary to suppress background signals. This was done using $^{13}C-^{13}C$ INADEQUATE and double quantum filtered $^{13}C-^{13}C$ DQF-COSY experiments. $^{13}C-^{13}C$ INADEQUATE spectra of oriented samples were acquired at 55.0 °C with a sweep width of 25 000 Hz, 2k complex points, 40 W decoupling power during acquisition (82 ms), a relaxation delay of 3.0 s, and with 8192 transients.

The $^{13}C-^{13}C$ DQF-COSY spectra of oriented samples were acquired at 48.0 °C using 20 W decoupling power during acquisition, a t_2 sweep width of 21739 Hz, 2K complex t_2 data points (94 ms acquisition time), 1.4 s pre-delay, 512 transients, 152 t_1 data points, and a t_1 sweep width of 2703 Hz. $^{13}C-^{13}C$ DQF-COSY spectra of isotropic samples were acquired in methanol-d_4 at 25.0 °C using 1 W decoupler power during acquisition, a 9804 Hz t_2 sweep width, 4k complex t_2 data points (418 ms acquisition time), 1.9 s pre-delay, 96 transients, 300 t_1 points, and a t_1 sweep width of 1562 Hz.

A systematic search of the entire glycosidic torsion conformational space (ϕ, ψ) was performed in terms of the residual dipolar coupling data with the aid of a computer program written in C.[3e] Fixed bond lengths and angles of the G_{M4} lactam analog were obtained from minimization with *MacroModel* (ver. 3.5X, W. C. Still, Columbia University). ϕ, ψ were varied independently in 2° increments, and square-well half-widths for the torsions were varied independently from 0° to 80° in 5° increments. Solutions from the program in which any single coupling differed from an experimental value by more than one full line width were excluded outright. Additionally, solutions were excluded in which the root mean square difference between the sets of fitted and experimental values exceeded half an average line width (18.5 Hz). The angles associated with the ϕ and ψ torsions are defined according to IUPAC convention.[14]

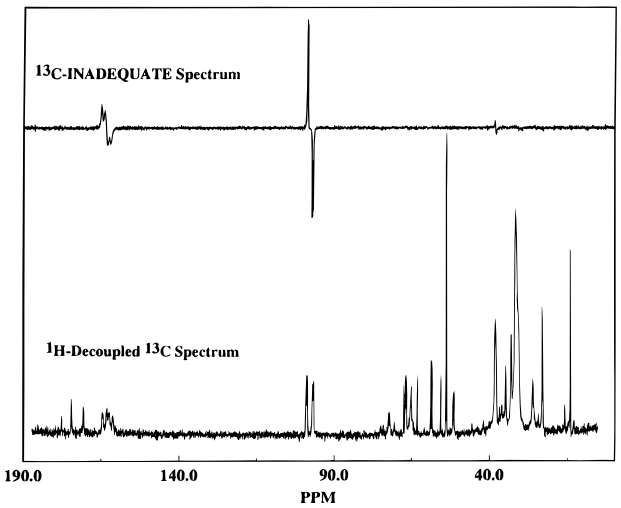

Figure 2. A proton-decoupled 1D ^{13}C-spectrum and 1D-INADEQUATE of G_{M4} lactam glycolipid (**3**) in DMPC/CHAPSO 3:1.

The FORTRAN program, ORDERTEN,[15] performed a systematic search of the order tensor elements to find those sets that reproduce the experimental NMR dipolar couplings. These were used to calculate chemical shifts for comparison with experimental values. These calculations require a static shift tensor, which can be obtained from literature or through *ab initio* methods. All *ab initio* calculations were performed on a Silicon Graphics INDY workstation, running a R4400 processor with 64 MB of RAM. The optimizations took approximately 6 h of CPU time, whereas the GIAO calculations took from 4 to 75 h of CPU time depending on the quality of the basis set used.

Results

NMR methods using ^{13}C-detection proved most useful in extracting dipolar coupling information from the labeled carbons in G_{M4} lactam within the DMPC/CHAPSO oriented micelle environment. Double quantum filtering through 1D-INADEQUATE ^{13}C-NMR very effectively eliminated natural abundance ^{13}C resonances from the lipid. Figure 2 illustrates both the 1D-^{13}C spectrum of G_{M4} lactam dissolved in DMPC/CHAPSO at 48.0 °C as well as the 1D-INADEQUATE spectrum. The chemical shifts of C_1, C_2, and C_3 of the sialic acid amide segment in the oriented sample can be seen in the 1D-^{13}C spectrum and were measured to be 162.2, 97.8, and 38.4 ppm, respectively. However, in the case of C_3, at least, the natural abundance peaks inhibit easy identification. The INADEQUATE experiment employs a $^{13}C-^{13}C$ double-quantum filter. This removes most natural abundance peaks because of the extremely low probability of having two adjacent ^{13}C sites, and C_3 then is easily identified at 38.4 ppm. The C_3 resonance is small by comparison with the other two signals in the INADEQUATE spectrum, because the C_2-C_3 coupling is small (∼20 Hz), and the filter delay in the INADEQUATE sequence is set to match the large C_1-C_2 coupling (∼250 Hz). Nevertheless, identification is straightforward.

It is noteworthy that these peaks are not exactly in the positions anticipated for the lactam dissolved in an isotropic solvent. This offset is particularly large for the carbonyl ^{13}C resonance due to the unusually large anisotropy for this atom.

(13) Levy, G. C.; Lichter, R. L. *Nitrogen-15 Nuclear Magnetic Resonance Spectroscopy*; JohnWiley & Sons: New York, 1979, p 32.

(14) International Union of Pure and Applied Chemistry *Pure Appl. Chem.* **1983**, *55*, 1269−1272.

(15) Sanders, C. R., II; Prestegard, J. H. *J. Am Chem. Soc.* **1992**, *114*, 7096−7107. (b) Sanders, C. R., II; Prestegard, J. H. *J. Am. Chem. Soc.* **1991**, *113*, 1987−1996.

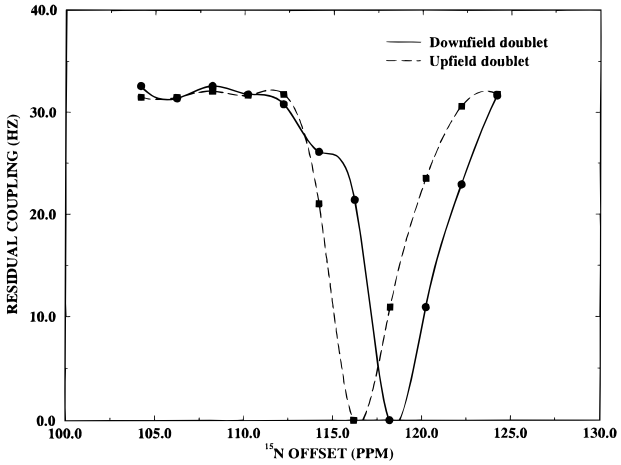

Figure 3. Plot of the residual C_2-N coupling ($J + D$) against the ^{15}N offset. Values for both the high- and low-field components of the C_2 resonance resulting from the C_1-C_2 coupling are shown. The ^{15}N chemical shift is in the middle of the points at which the two components of the C_1-C_2 doublet collapse (i.e. 117.4 ppm).

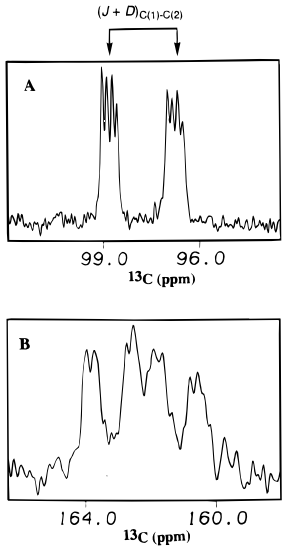

Figure 4. Expanded C_2 and C_1 multiplets (A and B, respectively) from the 1D-^{13}C spectrum of **3** in DMPC/CHAPSO 3:1. A total of five distinct experimental couplings ($J + D$) are measurable from these two multiplets.

In comparison to the lactam in an isotropic micellar phase consisting of DMPC/CHAPSO (16.0 °C), the chemical shift is 6.0 ppm upfield in the oriented phase (48.0 °C). These phases should have similar functional group distributions and hence similar perturbations of the chemical shifts. Thus, the resulting offsets reflect chemical shift anisotropy effects upon sample orientation and are of considerable utility in structural analysis. The chemical shift changes for C_2 and C_3 are smaller and therefore of less use in this application.

Orientational effects on ^{15}N are of similar value, but they are more difficult to observe directly because of the low magnetogyric ratio. It was possible to detect the isotropic chemical shift directly. However, due to line-broadening upon orientation, it was more practical to determine the chemical shift for ^{15}N upon orientation indirectly (through ^{13}C) by monitoring the collapse of the $^{15}N-^{13}C_2$ coupling as a function of the frequency of a weak ^{15}N rf field. This is depicted in Figure 3. The ^{15}N chemical shift value relative to 2.9 *M* NH_4Cl in 1.0 *M* HCl (referenced at 24.93 ppm) is 117.4 ppm. Again, a comparison can be made to the shift in an isotropic micellar system (114.4 ppm). The offset upon orientation is 3.0 ppm downfield. The same information could also have been obtained from a 2D $^{15}N-^{13}C$ correlation experiment.

Splittings due to the combination of dipolar and scalar couplings can be measured from expanded sections of the 1D-spectra. The observed couplings are a sum of dipolar and scalar components. Since the dipolar part can be large and of either sign, there is a much larger variation in coupling patterns than in solution spectra, which show only scalar couplings. Figure 4 illustrates blown-up views of multiplets for C_1 and C_2 from the 1D-^{13}C spectrum. The large coupling (255 Hz) is shared between the C_1 and C_2 multiplets and must belong to $(J+D)_{C1-C2}$. The intermediate coupling (40 Hz) in the C_2 multiplet is in-phase in the INADEQUATE spectrum and therefore must be $(J+D)_{C2-N}$. The smallest coupling in the C_2 multiplet (19 Hz) is shared with the C_3 resonance and is thus $(J+D)_{C2-C3}$. Two additional couplings within the C_1 multiplet are also apparent. One of these appears in-phase in the INADEQUATE and is thus $(J+D)_{C1-N}$ (154 Hz). The other one must therefore be $(J+D)_{C1-C3}$ (30 Hz). A total of three $^{13}C-^{13}C$ and two $^{15}N-^{13}C$ splittings were measured from these multiplets (Table 1).

Determination of the Signs of the Dipolar Couplings. The small C_2-C_3 splitting presumably results from the fact that the residual C_2-C_3 dipolar coupling is opposite in sign but nearly equal in magnitude to the normal scalar coupling of 64 Hz. As discussed above, the dipolar coupling components may be either positive or negative relative to the scalar terms. When dipolar terms dominate, the measured splittings can be either positive or negative. Knowing the sign of the measured residual splitting is important because, without it, two possible values of the dipolar contribution can exist. Each of these values corresponds to multiple values of the geometric variable θ in eq 1.

Table 1. Experimental Oriented and Isotropic Scalar Couplings

coupling	oriented couplings (Hz) ($\|J + D\|$)	isotropic couplings (Hz) (J)
C_1-N	154.4	−15.1
C_2-N	40.2	−6.2
C_1-C_2	255.2	63.6
C_2-C_3	19.4	44.0
C_1-C_3	30.5	0.0

It is possible to determine either the absolute sign of a dipolar coupling or the relative sign of a pair of couplings. The absolute sign of a coupling can be established by first knowing the scalar couplings and measuring the change in the observed couplings as the order of the sample is varied. For C_2-C_3, the observed coupling upon orientation ($J + D$) was smaller than the scalar coupling (J); this implied that J and D were of opposite sign. In addition, the observed coupling decreased as the sample order decreased, implying that the total splitting was negative (*i.e.* −19 Hz). Thus both the sign and magnitude of the C_2-C_3 residual dipolar coupling were readily established [*i.e.*, since $J_{C2-C3} = 44$ Hz $= (J+D = -19$ Hz), $D = -63$ Hz].

One experiment which proved highly useful in establishing the relative sign relationship for a pair of $^{13}C-^{15}N$ couplings (to the same ^{15}N) was a 2D $^{13}C-^{13}C$ DQF COSY. Multiplets in normal homonuclear COSY experiments give crosspeaks with components correlating every line of one multiplet with every line of a connected multiplet. For a three-spin system, half of these arise from a pulse-induced spin flip of a passive spin. When the passive spin is ^{15}N and a $^{13}C-^{13}C$ COSY is acquired, the ^{15}N spin is not flipped, and half the crosspeak components are missing. The position of these missing components identifies the relative sign of the ^{15}N coupling to the two carbons giving rise to the crosspeaks. This is illustrated in Figure 5, which shows one C_1-C_2 crosspeak from the $^{13}C-^{13}C$ DQF

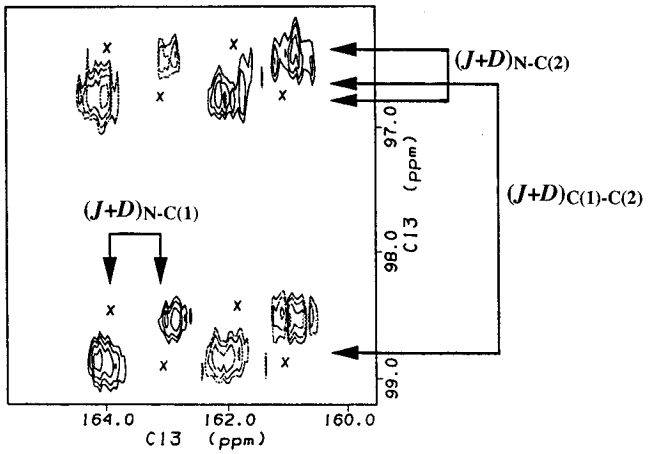

Figure 5. One C_1-C_2 cross peak from a double quantum-filtered $^{13}C-^{13}C$ COSY spectrum of **3** in DMPC/CHAPSO 3:1. The small x's indicate the complimentary set of possible peaks that would have appeared if the relative C_1-N to C_2-N sign relationship had been opposite.

COSY. Since each of the four identical pairs of ^{13}C crosspeaks with identical ^{15}N spin states lies parallel to the diagonal (not shown), the C_1-N and C_2-N couplings have the same sign. The complimentary set of peaks (which do not show up) are indicated by small x's. Had they shown up, instead, that would have been indicative of $C_1-^{15}N$ and $C_2-^{15}N$ being of opposite sign. Thus we were able to firmly establish that C_1-N and C_2-N were of the same sign.

The ^{15}N-spin-decoupling experiment, whose usefulness in establishing the ^{15}N chemical shift was described above, also allowed the determination of the relative signs of the C_1-C_2 and C_2-N couplings (Figure 3). Note that the $C_2-^{15}N$ doublet at higher ppm (*i.e.*, the downfield component of the C_1-C_2 doublet) collapsed to a null at a slightly higher decoupler offset than the upfield doublet. This was indicative of C_1-C_2 being of the opposite sign as C_2-N. Thus, it was possible to establish the relative sign relationship between two separate pairs of couplings and also the absolute sign of a single coupling. This narrowed the number of prospective sign sets for the five measured couplings from 32 to 4.

Analysis

Interpretation of the above dipolar splittings and CSA offsets was first attempted in terms of a bond-rotation model which includes both structural and motional parameters. The G_{M4} fused ring system itself was considered to be rigid but motion about the glycolipid torsion angles ϕ and ψ in wells of width $\Delta\phi$ and $\Delta\psi$ was allowed. The alkyl chain anchor was allowed to move in an axially symmetric manner about the bilayer normal characterized by S_{axial} as described above. The geometry for the rigid headgroup was represented by a minimized set of coordinates from *MacroModel.* These coordinates allow specification of various dipolar interactions in a molecular fixed frame and were fed, along with each of the possible sign sets for dipolar coupling, to a C program which performs a search for parameters that reproduce the splittings. Initially, only dipolar data were used because the CSA data are more easily analyzed in terms of order tensor elements than discrete ϕ and ψ rotations. The G_{M4} lactam headgroup was rotated through the complete conformational space to search for only those sets of ϕ and ψ torsions which reproduce the experimental dipolar couplings to within a reasonable error. Three separate families of structures were found. Table 2 illustrates both the experimental and calculated dipolar coupling values for each of the three families of structures. Representative structures (**I**, **II**, and **III**) from each of the three families are shown in Figure 6. The orientations of the glycerol side-chain and the acetyl group on the sialic acid have not been determined experimentally but have been shown as predicted in the *MacroModel* minimization. The ranges of torsion angles, well widths, and order parameters (ϕ, ψ, $\Delta\phi$, $\Delta\psi$, and S_{axial}) corresponding to each of these three structures are displayed in Table 3. The average ϕ and ψ torsions in these three structures differ greatly from each other.

Table 2. Measured and Predicted Residual Dipolar Couplings (D) for G_{M4}-Lactam Glycolipid (Structures **I**−**III**) in DMPC−CHAPSO (3:1) at 47.0 °C

coupling	measured D (Hz)[a]	predicted D (Hz)	difference (Hz)
	Structure I		
C_1-N	-139.3 ± 37	-118.0	21.3
C_2-N	-34.0 ± 12	-41.3	7.3
C_1-C_2	191.6 ± 12	185.8	5.8
C_2-C_3	-63.4 ± 12	-59.1	4.3
C_1-C_3	30.5 ± 18	50.9	20.4
	Structure II		
C_1-N	-139.3 ± 37	-121.8	17.5
C_2-N	-34.0 ± 12	-42.1	8.1
C_1-C_2	191.6 ± 12	183.7	7.9
C_2-C_3	-63.4 ± 12	-61.3	2.1
C_1-C_3	30.5 ± 18	53.3	22.8
	Structure III		
C_1-N	169.5 ± 37	160.0	9.5
C_2-N	46.4 ± 12	29.4	17.0
C_1-C_2	-318.8 ± 12	-319.4	0.6
C_2-C_3	-63.4 ± 12	-64.1	0.7
C_1-C_3	-30.5 ± 18	-38.0	7.5

[a] The errors were one half of the measured line widths.

Chemical Shift Anisotropy. To further assess each of the three possible structures, we turned to chemical shift anisotropy (CSA) effects. The observed chemical shift in a partially oriented system includes contributions from both the isotropic part of the chemical shift tensor and an anisotropic part due to the differential sampling of the various elements of the shift tensor (eq 2).[16] In order to interpret chemical shift anisotropy information in structural terms it is therefore necessary to have prior knowledge about the magnitudes and orientations of the principal shift tensor elements. This information may be obtained from model compounds containing an amide linkage.[17] However, our amide bond is in a somewhat unusual structural environment, and we felt it advisable to explore possible deviations using computational techniques. Over the past few years several *ab initio* methods for calculating chemical shifts have been developed[18] and applied in calculating chemical shifts for a large variety of molecules.[19] Several of these cases include peptide bonds.[20]

These calculations are computationally intensive, and we have attempted to reduce our system to the smallest acceptable model. Thus, calculations were performed on the fragment shown in Figure 7, which was considered to be a reasonable model for the headgroup of the G_{M4} lactam. Even with this reduction, however, the molecule's size makes it inconvenient to use extremely large basis sets. Therefore, we decided to use the GIAO method which seems to produce better results than other methods for small and medium-sized basis sets.[18g] This method has recently been effectively integrated into the *Gaussian95* suite of programs, thus allowing a direct SCF calculation, which is quite convenient when disk-space is limited.[21]

(16) Metz, G.; Howard, K. P.; van Liemt, W. B. S.; Prestegard, J. H.; Lugtenburg, J.; Smith, S. O. *J. Am. Chem. Soc.* **1995**, *117*, 564−565.
(17) Duncan, T. M. A Compilation of Chemical Shift Anisotropies; Farragut Press: Chicago, 1990.

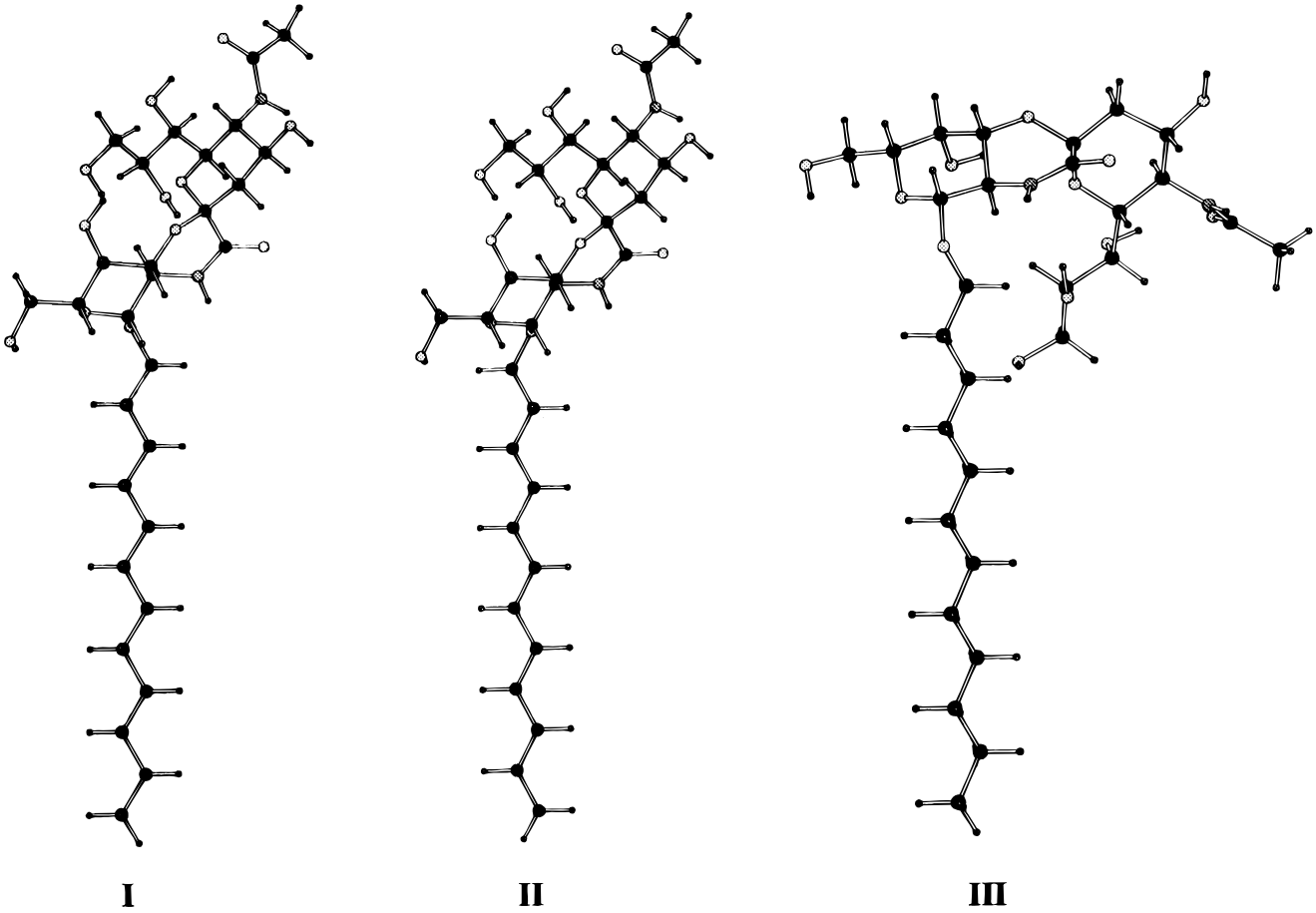

Figure 6. The structures **I**, **II**, and **III** consistent with the dipolar-coupling data. The lipid chain is perpendicular to the static magnetic field, B_o.

Table 3. Torsional Angles Determined from the Set of Experimental Dipolar Couplings

structure	ϕ	$\Delta\phi$	ψ	$\Delta\psi$	S_{axial}
I	−120° to −124°	(0° to 35°)	64 to 68°	(0° to 40°)	0.76 to 0.88
II	−56° to −62°	(0° to 35°)	−58° to −68°	(0° to 75°)	0.76 to 0.88
III	0° to 102°	(0° to 75°)	−104° to −258°	(0° to 75°)	0.64 to 0.88

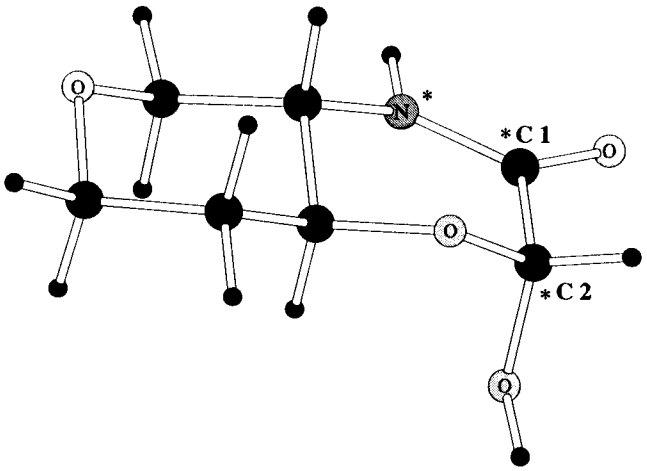

Figure 7. Structure of the *ab initio* model fragment optimized at the HF/3-21G level.

The model fragment was optimized at a HF/3-21G level. This level of theory has been shown to reproduce experimental geometries reasonably well, though energies obtained are far from accurate.[22] GIAO calculations were performed on the optimized fragment using a large number of basis sets ranging from the medium-sized 6-31G* to the fairly large 6-311++G-(2d,2p) basis sets.[23] Optimization and GIAO calculations were also performed on methane (^{13}C reference) and ammonia (^{15}N reference) at corresponding levels of theory.

(18) (a) Kutzelnigg, W. *J. Mol. Struct. (Theochem)* **1989**, *202*, 11−61. (b) Chestnut, D. B. *Annu. Rep. NMR Spectrosc.* **1989**, *21*, 51−97. (c) Kutzelnigg, W. *Isr. J. Chem.* **1980**, *19*, 193−200. (d) Schindler, M.; Kutzelnigg, W. *J. Chem. Phys.* **1982**, *76*, 1919−1933. (e) Hansen, A. E.; Bouman, T. D. *J. Chem. Phys.* **1985**, *82*, 5035−5047. (f) Ditchfield, R. Molec. Phys. **1974**, *27*, 789−807. (g) Wolinski, K.; Hinton, J. F.; Pulay, P. *J. Am. Chem. Soc.* **1990**, *112*, 8251−8260. (h) Fukui, H.; Miura, K.; Yamazaki, H.; Nosaka, T. *J. Chem. Phys.* **1985**, *82*, 1410−1412.

(19) (a) Barfield, M.; Yamamura, S. H. *J. Am. Chem. Soc.* **1990**, *112*, 4747−4758. (b) Barfield, M. *J. Am. Chem. Soc.* **1993**, *115*, 6916−6928. (c) Schindler, M. *J. Am. Chem. Soc.* **1988**, *110*, 6623−6630. (d) Ghose, R.; Marino, J. P.; Wiberg, K. B.; Prestegard, J. H. *J. Am. Chem. Soc.* **1994**, *116*, 8827−8828.

(20) (a) Lumsden, M. D.; Wasylishen, R. E.; Eichele, K.; Schindler, M.; Penner, G. H.; Power, W. P.; Curtis, R. D. *J. Am. Chem. Soc.* **1994**, *116*, 1403−1413. (b) Jiao, D.; Barfield, M.; Hruby, V. J. *J. Am. Chem. Soc.* **1993**, *115*, 10883−10887. (c) de Dios, A. C.; Oldfield, E. *J. Am. Chem. Soc.* **1994**, *116*, 11485−11488.

(21) Frisch, M. J.; Trucks, G. W.; Schlegel, H. B.; Gill, P. M. W.; Johnson, B. G.; Robb, M. A.; Cheeseman, J. R.; Keith, T.; Petersson, G. A.; Montgomery, J. A.; Raghavachari, K.; Al-Laham, M. A.; Zakrzewski, V. G.; Ortiz, J. V.; Foresman, J. B.; Cioslowski, J.; Stefanov, B. B.; Nanayakkara, A.; Challacombe, M.; Peng, C. Y.; Ayala, P. Y.; Chen, W.; Wong, M. W.; Andres, J. L.; Replogle, E. S.; Gomperts, R.; Martin, R. L.; Fox, D. J.; Binkley, J. S.; Defrees, D. J.; Baker, J.; Stewart, J. P.; Head-Gordon, M.; Gonzalez, C.; Pople, J. A. *Gaussian 95 (Development Version) Revision B.1*; Gaussian Inc.: Pittsburgh, PA, 1995.

(22) Head-Gordon, T.; Head-Gordon, M.; Frisch, M. J.; Brooks, C. L., III; Pople, J. A. *J. Am. Chem. Soc.* **1991**, *113*, 5989−5997.

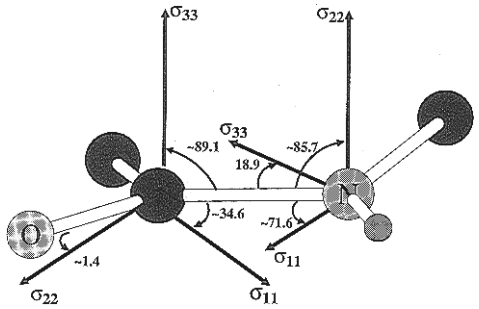

Figure 8. The calculated orientations of the ^{13}C and ^{15}N shift tensors in the laboratory frame. Orientations depicted are those calculated using the GIAO/6-31G* basis set, but these varied little for different basis sets, as mentioned in the text. A common reference frame was defined to relate the shift tensor and order tensor elements, such that C(α)−C(O) is coincident with the *x*-axis and the *z*-axis is perpendicular to the O═C−N plane.

The magnitudes of the principal elements for ^{13}C did not seem to vary significantly with the size of the basis set (∼8%). However the principal elements of the amide ^{15}N shift tensor seemed to be more sensitive to basis set size (∼25% variation), this is only to be expected since diffuse functions in *sp*-space have been shown to be important in systems involving lone pairs.[23] The orientations of the principal components for either ^{13}C or ^{15}N do not seem to be significantly affected by variation in the quality of the basis set (changes being in the order of 1.5°). The results obtained for our smallest, 6-31G* and largest, 6-311++G(2d,2p) basis sets are shown in Table 4. Orientations of the principle axes of the shift tensor for both the ^{13}C and ^{15}N nuclei for the 6-31G* basis set are shown in Figure 8.

The calculated shift tensors seemed to differ little in magnitude and orientation from experimental data in the literature for ^{13}C, with the differences in magnitude being less than 10% and the differences in orientation being even smaller. In the case of the ^{15}N shift tensors, the magnitudes seemed to deviate by around 30% from various experimental determinations, but the differences in orientation were again small. Deviations of the observed isotropic shifts from calculated values may be due to one or more effects which we neglect in our analysis. The presence of the bilayer would certainly perturb the chemical shifts, along with other neighboring groups and environmental effects. Chemical shifts have been shown to be sensitive to electric fields and field gradients.[24] Inadequacies in choosing the model and the basis set could also contribute to the aforementioned minor differences. While differences between experimental and calculated tensors are not large, we use calculated shift tensors in what follows because they would be expected to reflect local bond interactions in our lactam better than the available experimental data on peptides.

The calculated shift tensor information was ultimately used to differentiate between structures **I**, **II**, and **III**. Visually, structures **I** and **II** have the same upright headgroup orientation. This orientation is strikingly different from the one in structure **III**, in which the headgroup lies along the membrane. Based on this difference and the magnitudes and orientations of the calculated shift tensors, it was anticipated that chemical shift anisotropy (CSA) effects in structure **III** would differ greatly from those in structures **I** and **II**. For example, the most shielded element of the ^{13}C chemical shift tensor lies perpendicular to the plane of the amide. We would thus anticipate an upfield shift upon orientation for structures **I** and **II**, in which this vector is partly aligned with the magnetic field. In structure **III**, however, this vector would lie nearly along the bilayer normal and would always be perpendicular to the field. This would result in a downfield shift upon orientation.

Table 4. Calculated Principal Components of the $^{13}C^a$ and $^{15}N^b$ Shift Tensor

	basis set	δ_{11} (ppm)	δ_{22} (ppm)	δ_{33} (ppm)	iso (ppm)
^{13}C	6-31G*	260.2	159.6	76.2	165.3
	6-311++G(2d,2p)	280.1	170.6	83.7	178.1
^{15}N	6-31G*	173.2	76.0	22.3	90.5
	6-311++G(2d,2p)	197.9	90.4	30.6	106.3

[a] Shifts referenced to CH_4 $\delta_{ref} = 201.2$ for 6-31G* and 197.0 for 6-311++G(2d,2p)]. [b] Shifts referenced to NH_3 $\delta_{ref} = 267.04$ for 6-31G* and 265.08 for 6-311++G(2d,2p)].

Table 5. Predicted and Observed Chemical Shift Changes upon Orientation

structure	basis set	^{13}C (ppm)	^{15}N (ppm)
I and **II**	6-31G*	−8.7	3.9
I and **II**	6-311++G(2d,2p)	−6.1	4.1
III	6-31G*	12.9	0.7
III	6-311++G(2d,2p)	8.4	0.8
obsd		−6.0	3.0

Quantitatively predicting orientation-dependent shift offsets can, in principle, be done from the parameters producing best fits to dipolar data. In practice, it is easier to combine the effects of ϕ, ψ, $\Delta\phi$, $\Delta\psi$, and S_{axial} in a general order tensor, which also has five independent elements. This was done by refitting data with a search over order tensor elements. When the tensors were diagonalized to orient the order frame in the molecular frame, two distinct headgroup orientations were found, with one matching that obtained from the torsional analysis for structures **I** and **II** and another corresponding to **III**. The predicted changes in shifts were then calculated using the order tensor elements and the calculated chemical shift tensor elements as described in eq 3. The results are compared to the measured values in Table 5. Structures **I** and **II** fit the observation well, whereas structure **III** would have produced shifts in the opposite direction upon orientation.

Discussion

As detailed in the previous section, the combined use of NMR dipolar coupling and chemical shift measurements provided a single reasonable picture of the G_{M4} lactam headgroup orientation in a membrane environment. In both structures **I** and **II**, the headgroup is extended out away from the surface of the membrane in a virtually identical manner. However, an argument can be made for structure **II** over structure **I**. First, the lipid chain C_1−O bond in **I** eclipses the anomeric C−H bond in the galactose ring. This is clearly less favorable than the gauche conformation for the corresponding bonds in **II**. Structure **II** is also favored by arguments invoking the exo-anomeric effect, since one of the lone pairs on the oxygen atom outside the ring is aligned anti-periplanar to the C−O bond within the ring.[25] In **I**, there is no such favorable alignment.

The conformation in structure **II** is consistent with previous studies of β-linked oligosaccharides in a model membrane environment in several respects. First, the preferred values of ϕ and ψ fall in regions consistent with structures for β-linked glycosides as found in crystallographic[26] and solution NMR[25,27]

(23) Frisch, M. J.; Pople, J. A.; Binkley, J. S. *J. Chem. Phys.* **1984**, *80*, 3265−3269.

(24) (a) de Dios, A. C.; Pearson, J. G.; Oldfield, E. *Science* **1993**, *260*, 1491−1496. (b) Pearson, J. G.; Oldfield, E.; Lee, F. S.; Warshel, A. *J. Am. Chem. Soc.* **1993**, *115*, 6851−6862.

(25) Thogersen, H.; Lemieux, R. U.; Bock, K.; Meyer, B. *Can. J. Chem.* **1982**, *60*, 44−57.

(26) Jeffrey, G. A. *Acta Crystallogr., Section B* **1990**, *B46*, 89−103.

(27) van Halbeek, H. *Curr. Opinion Struct. Biol.* **1994**, *4*, 697−709.

structural studies as well as in molecular modeling calculations.[28] As mentioned above, the ϕ value of around $-60°$ is also consistent with earlier predictions based on the exo-anomeric effect.[25] Second, the motional freedom which allows the headgroup to adopt other orientations actually appears quite limited. S_{axial} is large (0.7−0.9) and not too different from typical order parameters for parts of phospholipids near the membrane interface (*e.g.*, 0.65 for the C_2 carbon of phospholipid acyl chains).[29] The range of torsional well widths used to model motion about the average values of both ϕ and ψ angles for structure **II** is small for $\Delta\phi$ [$\pm$(0−35°)] but moderately large for $\Delta\psi$ [$\pm$(0−75°)]. This compares favorably with the range of torsional well widths found for a similar alkyl glycoside, β-dodecyl glucoside.[3e] Third, the overall structure is one in which the bulk of the headgroup is extended away from the membrane interface. This observation has been made in several previous studies by our group[3a] and others,[30] and it indicates that protein/carbohydrate interactions involving this molecule (and the corresponding lactone) would likely involve structural contacts with the peripheral part of the sialic acid moiety. In particular, the C_7−C_9 glycerol chain and the *N*-acetyl group are the most exposed portions of the molecule. The lactam amide bond, which replaces the natural lactone, actually points back toward the membrane surface and is buried near the membrane surface.

The exposure of the *N*-acetyl and glycerol portions of the sialic acid is interesting. The actual physiologically important proteins which might use ganglioside lactones as receptors in mammals are not known. However, several proteins are known to interact with sialic acid-terminated carbohydrate chains, among them wheat germ agglutinin[31] (a plant lectin) and hemagglutinin,[32] a viral protein. In both cases, it is the *N*-acetyl moiety of the sialic acid instead of the carboxyl group which is most intimately involved in binding.

Aside from structural implications, the methodology employed here offers some promise for the future. In particular, chemical shift offsets due to anisotropies in the ^{15}N and ^{13}C shift tensors for amides have been critical in distinguishing between conformational possibilities. The interpretation of ^{15}N shift tensors has proven advantageous in structural analysis of membrane associated peptides in the past,[33] and there are some applications of ^{13}C shift tensors with carbohydrates.[3c] However, the use of ^{15}N tensors in the study of cell surface carbohydrates is new, and the widespread occurrence of *N*-acetyl groups in other carbohydrates points to other potential applications. We have used chemical shift effects here as an additional screening factor, but, in the future, this information could easily be incorporated directly into a structure-search protocol.

Acknowledgment. We would like to thank Prof. Kenneth Wiberg for assistance with *ab initio* calculations and Dr. Kathleen Howard for useful discussions. This work was supported by the National Institutes of Health, Grant GM33225 and also by a post-doctoral fellowship from the National Cancer Institute for Dr. B. A. Salvatore (Fellowship No. 1 F32 CA59254-01 BIOM).

JA9540482

(28) Howard, K. P. Ph.D. Thesis, Yale University, 1995.

(29) (a) Gally, H. U.; Pluschke, G.; Overath, P.; Seelig, J. *Biochemistry* **1981**, *20*, 1826−1831. (b) Strenk, L. M.; Westerman, P. W.; Doane, J. W.; *Biophys. J.* **1985**, *48*, 765−773.

(30) (a) Renou, J.-P.; Giziewicz, J. B.; Smith, I. C. P.; Jarrel, H. C. *J. Am. Chem. Soc.* **1989**, *28*, 1804−1814. (b) Nyholm, P.-G.; Pascher, I. *Biochemistry* **1993**, *32*, 1225−1234.

(31) Lis, H.; Sharon, N. *Annu. Rev. Biochem.* **1986**, *55*, 35−67.

(32) Rini, J. M. *Annu. Rev. Biophys. Biomol. Struct.* **1995**, *24*, 551−577.

(33) (a) Cross, T. A.; Opella, S. J. *Curr. Opin. Struc. Biol.* **1994**, *4*, 574−581. (b) Mai, W.; Hu, W.; Wang, C.; Cross, T. A. *Protein Sci.* **1993**, *2*, 532−542. (c) Teng, Q.; Cross, T. A. *J. Magn. Reson.* **1989**, *85*, 439−447.